Effect of temperature on the dynamics of electron transfer in heterogeneous medium: Evidence for apparent Marcus inversion

Manoj Kumbhakar, Sukhendu Nath, Tulsi Mukherjee, Haridas Pal *

Radiation & Photochemistry Division, Bhabha Atomic Research Centre, Mumbai 400085, India

Abstract

Temperature effect on electron transfer (ET) rates in coumarin–aromatic amine systems have been investigated in TX-100 micellar solution using fluorescence quenching measurements. Interesting observation in the present systems is the appearance of Marcus inversion in ET rates at unexpectedly lower exergonicity, which we explain on the basis of the two-dimensional ET (2DET) theory. Temperature dependent results in the present systems indicate substantial activation barrier, not only in the normal Marcus region, but also in the inverted region as well as at the maximum of the Marcus correlation curve. Because of the involvement of the nuclear tunneling via the participation of high frequency vibrational modes, temperature effects are usually not expected in the true inverted region. It is inferred from the present results that the Marcus inversion observed in the present systems is actually an apparent inversion, arising at exergonicities much lower than the true barrierless situation, and consequently show strong temperature effect. On the basis of the 2DET theory, the apparent inversion in these systems is understood to occur due to persistent nonequilibrium solvation for the reactant state along solvation axis during the progress of the ET reaction along intramolecular coordinate. Observed temperature effect supports the applicability of 2DET theory and also justifies the observed inversion in the ET rates at unexpectedly lower exergonicities. Present results demonstrate the observation of apparent Marcus inversion even when the ET reactions are in the normal exergonicity region ($-\Delta G^0 < \lambda_s$).
© 2006 Elsevier B.V. All rights reserved.

Keywords: Photoinduced electron transfer; Marcus inversion; Two dimensional electron transfer theory; Coumarins; Aromatic amines; Triton X-100; Apparent inversion

1. Introduction

Extensive studies have been carried out on electron transfer (ET) processes in homogeneous media to understand the details of the mechanisms and dynamics of the ET reactions in different systems. From theoretical viewpoint, the most important feature of the outer-sphere ET reactions is the predicted inversion in the ET rates at higher exergonicities, which is universally known as the Marcus inversion [1–15]. Though the predicted Marcus inversion remained a controversy for more than about two decades since its prediction in 1956 [14,15], at present there are several experimental demonstrations of this unique behavior in homogeneous solutions, showing clear inversion in the Marcus correlation plots for the ET rates with the exergonicity of the reactions. Most of these experimental evidences for Marcus

inversion are, however, observed for the intramolecular ET reactions where the donors and acceptors are directly connected by chemical bonds [16–21]. Another important class of the ET reactions, where Marcus inversion behavior has also been observed in many systems, is the charge recombination (CR) reactions in contact ion-pair (CIP) states [22–27]. Contrary to the above systems, reports on Marcus inversion in bimolecular ET reactions are not only very rare but are also not that convincing in most cases [28,29], except the reports of Guldi and co-workers for some ET systems involving fullerens as the reactants [30,31] and slow electron transfer across zeolite–solution interface by Fukuzumi et al. [32].

Though extensive studies have been performed on the ET reactions in homogeneous solutions, similar studies in heterogeneous media, e.g. micelles, reverse micelles, proteins, DNA's, etc., are not that extensive [33–38]. Studies on the ET reactions in heterogeneous media are reported to have a relevance to the applications like solar energy conversion and its storage, especially in suppressing the energy wasting back electron trans-

fer (BET) processes between the primary ET products [37,38]. Among different heterogeneous media, micellar solutions have drawn considerable interest of the researchers to investigate the effect of the topology of the heterogeneous reaction media on the kinetics and mechanisms of different chemical reactions [37,38]. In our recent studies on bimolecular ET reactions in micellar media we have observed clear inversion in the Marcus correlation of the ET rates with the free energy (ΔG^0) changes of the reactions [39–41]. In these studies, it is interestingly seen that the maxima in the Marcus correlation curves appear at an exergonicity ($-\Delta G^0$) that is substantially lower than even the solvent reorganization energy λ_s [39–41]. To be mentioned that from conventional ET theories [1–15], where solvation coordinate (X) is effectively considered as the reaction coordinate for the ET process, the maxima in the Marcus correlation curves should appear at the barrierless condition of $-\Delta G^0 = \lambda_s + \lambda_i$, where λ_s and λ_i are the solvent and intramolecular reorganization energies, respectively. In our micellar ET studies [39–41], as the onset of the Marcus inversion appears at an unusually lower exergonicity than expected from conventional ET theory, we explained this observation qualitatively on the basis of slower relaxation along solvent coordinate (X) in these systems in comparison to the rate of ET reaction along the intramolecular coordinate (q), a concept introduced in the well-known two-dimensional ET (2DET) theory by Sumi and Marcus [42]. According to 2DET theory, the maximum in the Marcus correlation curves can appear at an exergonicity lower than the true barrier-less situation ($-\Delta G^0 = \lambda_s + \lambda_i$), if the reactant state is produced substantially away from the equilibrium solvation coordinate ($X = 0$) and the state is restricted to remain there during the ET reaction along the nuclear coordinate q [39–41]. Heterogeneous media like micelles where solvent relaxation dynamics is unusually slow, above condition is satisfied to a large extent, and thus Marcus inversion can be observed at reasonably lower exergonicities [39–41]. To be mentioned in the present context that Fukuzumi et al. [43] also observed Marcus inversion in bimolecular ET reactions in heterogeneous systems like DNA intercalated dyes, where the maximum in the Marcus correlation curve is apparently shifted to an unexpectedly lower exergonicity, an observation quite similar to ours for the bimolecular ET reactions in micellar solutions [39–41].

Though the observed inversion behavior for the bimolecular ET rates in micellar media could be qualitatively explained on the basis of the 2DET theory [39–41], more studies are required to understand further details of the ET reactions in these systems, especially to find supportive evidences for the applicability of 2DET model. With this aim, in the present work we have investigated the temperature effect on the bimolecular ET reactions between coumarin acceptors and aromatic amine donors in nonionic triton X-100 (TX-100) micellar solution. The donor–acceptor pairs used in this work are similar to those used in our earlier study, where Marcus inversion was observed [40]. In the present work, TX-100 micelle has been chosen as the reaction medium as the charactaristics of this micelle are well reported as a function of temperature [44,45]. Chemical structures of the acceptors (coumarin dyes) and donors (aromatic amines) used in the present work are shown in Scheme 1.

Coumarins (Acceptors):

(C151)   (C152)   (C481)
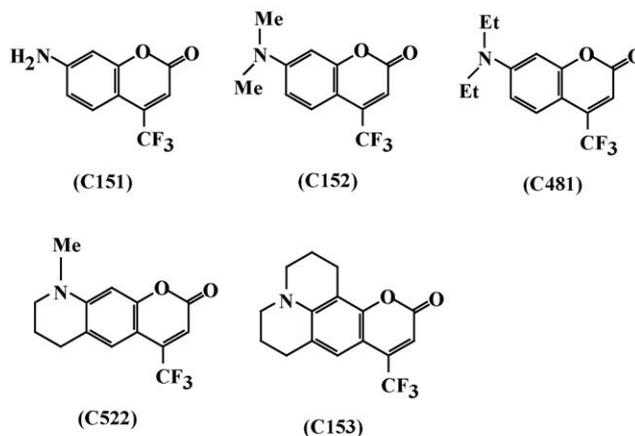
(C522)   (C153)

Aliphatic Amines (Donors):

DMAN   DEAN
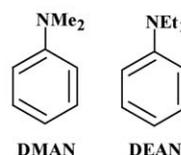
Scheme 1.

2. Experimental

Laser grade coumarin dyes {viz. coumarin-151 (C151), coumarin-152 (C152), coumarin-481 (C481), coumarin-522 (C522) and coumarin-153 (C153)} were obtained from Exciton, USA. Aromatic amines {viz. *N,N*-diethylaniline (DEAN) and *N,N*-dimethylaniline (DMAN)} were obtained from Spectrochem (India) or Qualigens Fine Chemicals (India) and were purified by vacuum distillation just before use. TX-100 was obtained from BDH and used as received. Nanopure water, having a conductivity of $\sim 0.1\ \mu S\ cm^{-1}$, was obtained by passing distilled water through a Barnstead Nanopure Water System and used for the preparation of the micellar solutions.

A JASCO UV–vis spectrophotometer, model V-530, was used for all the absorption measurements. A Hitachi spectrofluorometer, model-4010, was used for all the steady-state fluorescence measurements. A time-resolved fluorescence spectrometer from IBH, UK, which works on the principle of time-correlated single photon counting, was used for the measurements of the fluorescence decays. In the present work, a 408 nm diode laser (<100 ps, 1 MHz) was used as the excitation light source and a TBX4 detection module (IBH) coupled with a special Hamamatsu PMT was used for fluorescence detection. For the present setup, the instrument response function was ~ 240 ps at FWHM. Fluorescence decays were recorded with a vertically polarized excitation beam and fluorescence was collected at magic angle (54.7°). In the present measurements, temperature of the solution was adjusted and controlled within an accuracy of $\pm 1\,°C$, with the help of a cold-finger arrangement and using a microprocessor based temperature controller (model DS) from IBH.

3. Results and discussion

3.1. Estimation of the bimolecular quenching constants

In the present work the concentration of TX-100 micelle in the solution was kept around 1 mM and that of the coumarin dyes in the solution were kept about 100 times lower (around 10 μM) than that of the micelles in the solution. With this experimental condition, only a small fraction of the micelles can have a coumarin molecule in it, and following Poisson distribution [46] the probability of a single micelle containing more than one coumarin molecules is just negligible. In the present studies, the concentrations of amines were, however, varied over a wide range, from 0 to about 50 mM, such that each micelle can even have much more than one quencher molecules at the higher amine concentration range. The temperature of the solution was varied in the temperature range of 288–303 K. As reported in the literature, aggregation number and radius of the TX-100 micelle changes almost linearly for the temperature range of about 283–313 K [44,45]. Thus, in present work temperature variation was restricted well within the above range to ascertain the stability and integrity of spherical TX-100 micelles in the solution [44,45]. The relevant micellar parameters at different temperatures are listed in Table 1 [44,45,47].

As the volume of each micelle is restricted by the micellar boundary, assuming that the amine molecules mainly solubilised in the micellar phase, which is in fact expected because of the insolubility of the aromatic amines in pure water, the effective concentration of the amine quenchers in the micelles will be much higher than the total concentration used in the solution. As suggested in the literatures [33,34], aromatic amines mainly reside in the micellar Palisade layer. Therefore, the effective concentration of the amine quenchers in the micellar Palisade layer was calculated using the following relation [39–41]:

$$[Q]_{\text{eff}} = \frac{N_{\text{ag}}[Q]_{\text{t}}}{V_{\text{PL}}\{[S]_{\text{t}} - \text{CMC}\}} \tag{1}$$

where N_{ag} is the micellar aggregation number, V_{PL} is volume of the micellar Palisade layer, $[S]_{\text{t}}$ is the total TX-100 surfactant concentration used, $[Q]_{\text{t}}$ is the total amine concentration used in the solution and CMC is the critical micellar concentration. The volume of the Palisade layer was estimated from the knowledge of the radius of the micelle and that of the micellar core (cf. Table 1). For the present work, the radius of the micellar core is approximated to be ∼25 Å [47] for all the temperatures studied. As reported in the literature, the increase in the size of

TX-100 micelle with temperature is mainly due to an increase in the micellar hydration and aggregation number [44,45], and the increased micellar hydration is expected to cause mainly an expansion of the micellar Palisade layer, without causing much effect on the size of the nonpolar micellar core.

In our earlier studies, it was established that in micellar solution the coumarin dyes preferably reside in the micellar Palisade layer [39,40,48,49]. In the present work, absorption spectra of all the coumarin dyes in TX-100 micellar solutions were recorded, both in the absence and in the presence of amines. It is observed that the absorption characteristics of the coumarin dyes remain almost unchanged even in the presence of quite high amine concentrations used. These results indicate that there is no significant ground state complex formation between the coumarin dyes and the amine quenchers used [39–41].

Fluorescence spectra of the coumarin dyes in TX-100 micelles were recorded at different temperatures in the absence and presence of different concentrations of the amines. In the absence of amines, no appreciable change in the spectral shape and intensity was observed on changing the temperature of the solution in the range of 288–308 K. These results suggest that for the above temperature range the probe in the micelle experiences almost similar polarity for the microenvironment around it [49]. It is, however, seen that, at all the temperatures studied, the fluorescence intensity of the coumarin dyes in TX-100 micelle undergoes substantial quenching in the presence of the amines. A comparison of the fluorescence spectra of the coumarin dyes in the micellar solution in the absence and presence of amines indicates that there is no observable change in the emission spectral characteristics even in the presence of quite high concentration of the amines used. This excludes the formation of any exciplex or emissive charge transfer (CT) complex between the excited coumarin dyes and the ground state amine quenchers [50]. At all the temperatures studied, the Stern–Volmer plots, as obtained from steady-state quenching results, always show a positive deviation at higher quencher concentrations, indicating the presence of substantial static-quenching [50]. Similar observations were also made in our earlier works in the micellar ET reactions at room temperature, and attributed to the close contact donor–acceptor pairs at high quencher concentrations, which undergo almost instantaneous quenching following the photoexcitation of the dyes [39–41]. Due to this strong static-quenching, it is obvious that the estimated quenching rate constants (k_q^{SS}) from the steady-state results will always have some static-quenching contribution. Thus, in correlating the ET kinetics in the present systems with free energy changes (ΔG^0) of the ET reactions, as will be discussed in the next section, we avoid these k_q^{SS} values, but used the quenching constants k_q^{TR} estimated from the TR measurements [39–41], as are discussed below.

The time dependent quenching studies for the excited coumarin dyes by the amine donors were carried out by measuring the fluorescence decays of the dyes in TX-100 micelle at different temperatures in the presence of different concentration of the amines. It is found that at all the temperatures studied, the coumarin dyes show single exponential decays in the micellar solution in the absence of the amines. Addition of the amines to the solution, however, is seen to cause an enhance-

Table 1
Micellar parameters of TX-100 at different temperatures

Temperature (K)	CMC (mM)	N_{agg}	r_{micelle} (Å)	$\langle \tau_{\text{s}} \rangle$ (ns) [48]
288	0.334	48	37	1.28
293	0.327	64	38	
298	0.319	86	44	1.93
303	0.306	112	49	
308	0.294	150	54	1.04

For all the temperature the micellar core radius was considered to be 25 Å [46].

ment in the fluorescence decay rates, indicating the presence of dynamic interaction between the excited dyes and the amine quenchers. Moreover, in the presence of amines, the fluorescence decays of the coumarin dyes are seen to display clear nonsingle-exponential behavior [39–41].

Fluorescence quenching kinetics in micellar solution have been the subject of long lasting research interest, and a number of kinetic models have been proposed to account the nature of the decays of the excited fluorophores in the presence of quenchers in the micellar solutions [51–55]. In these models, the reactants can freely diffuse in the micelle and can also undergo exchange between the micellar and the aqueous phases. As the acceptors and donors used in the present work are almost insoluble in water, they will mainly reside within the micellar phase [39–41]. The fluorescence lifetimes of the coumarin dyes used are all in the nanosecond range ($\sim$2 to $\sim$5 ns). Thus, during the excited state lifetime, the exit and entry of the reactants in the micelles, which mostly occur in the microsecond time scale [51–55], will have effectively no effect on the observed quenching kinetics [39–41]. Due to orderliness and considerable rigidity within the micelle, the diffusion of the reactants inside the micelle will be much slower than in a homogeneous solution [39–41]. Comparing the microviscosity of the micellar Palisade layer ($\eta \sim 26$ cP [56]), with the viscosity of homogeneous solvent acetonitrile ($\eta \sim 0.345$ cP [57]), the diffusional rate constant k_d in micellar Palisade layer ($\sim 2 \times 10^8$ dm^3 mol^{-1} s^{-1}) is expected to be about two order of magnitude lower than in acetonitrile solution ($\sim 1.5 \times 10^{10}$ dm^3 mol^{-1} s^{-1} [58,59]). Thus, it is evident that in the present systems the quenching interaction occurs much faster (nanoseconds) than the diffusion of the reactants in the Palisade layer. Therefore, the common diffusional quenching kinetic model is not applicable for the present systems. Due to slow diffusion of the reactants, the quenching interaction in the present systems can be better visualized as equivalent to intermolecular interactions under nondiffusive conditions, and the distant dependent distribution of the amine quenchers around excited coumarin dyes will effectively determine the observed quenching kinetics [39–41]. Accordingly, the fluorescence decays of the coumarin dyes in the presence of amine quenchers are expected to show nonexponential behavior [39–41]. In a recent report on long-range electron transfer across zeolite–solution interface, Fukuzumi et al. [32] have also observed multiexponential kinetics. These authors have thoroughly considered the distance dispersion of the donors and acceptors in the heterogeneous media while calculating the average rates of electron transfer [32], following an approach similar to that of Albery et al. [60]. In this context, approach of Fayer and co-workers in the analysis of multiexponential kinetics in micellar media is also worth mentioning [33–36], although these authors assumed the diffusion of the reactants in the micellar phase. In the present systems, other than the distance dependent distribution of the quenchers, multiexponential fluorescence decay is also expected due to slower solvent relaxation than the electron transfer process [39–41], as discussed in the two-dimensional electron transfer model [42]. Therefore, a detailed analysis of the observed fluorescence decays implicitly considering the effects of the distance dependent distribution

of the quenchers and the slower solvation process is extremely complicated. In the present work, we thus adopted a very simple approach to estimate the average quenching constants based on the multiexponential analysis of the decays. Assuming that the average lifetime (τ_{av}) of the coumarin dyes decreases more or less linearly with the effective quencher concentration, τ_{av} can be expressed as,

$$(\tau_{av})^{-1} \approx k_0 + k_q^{TR}[Q]_{eff} \qquad (2)$$

where k_q^{TR} is the effective quenching constant. Under this situation, measuring the τ_{av} values of the coumarin dyes in the presence of different quencher concentrations, the k_q^{TR} can be estimated using the standard Stern–Volmer relation as [50],

$$\frac{\tau_0}{\tau_{av}} = 1 + k_q^{TR}\tau_0[Q]_{eff} \qquad (3)$$

In the present work, we tried to fit the observed decays following multiexponential analysis and use the fitting parameters thus obtained to estimate the τ_{av} values of the coumarin dyes in the presence of different amine concentrations [39–41]. For the present systems, it is seen that the observed decays fit reasonably well with a bi-exponential function. Thus, τ_{av} values were estimated as [39–41],

$$\tau_{av} = \frac{1}{100}(A_1\tau_1 + A_2\tau_2) \qquad (4)$$

where τ_1 and τ_2 are the respective lifetimes of the fast and slow components of the fluorescence decays and A_1 and A_2 are their respective percentage contributions, as obtained from the bi-exponential analysis of the observed fluorescence decays. It is seen that for all the coumarin–amine pairs, the τ_{av} gradually decreases with an increase in the amine concentration and follows a linear SV relation (cf. Eq. (3)) within the experimental error. Typical Stern–Volmer plots for C153–DMAN system at different temperatures are shown in Fig. 1. Similar plots were also obtained for other coumarin–amine pairs. Interesting point to note that unlike the steady-state results, the Stern–Volmer plots obtained from TR measurements are reasonably linear for
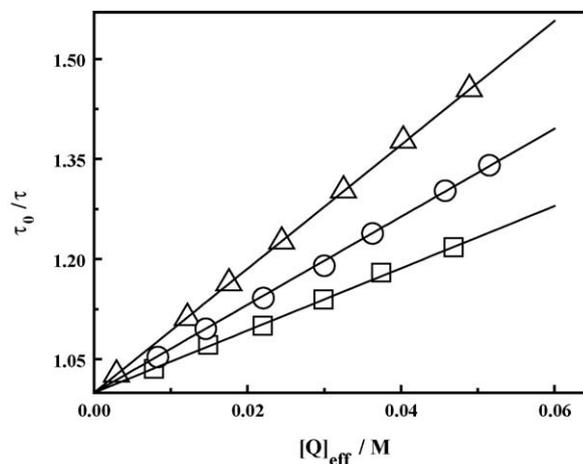

Fig. 1. Stern–Volmer plot for C153–DMAN system in TX-100 micellar solution at 288 ($\square$), 298 ($\bigcirc$) and 308 K ($\triangle$). Lifetime of C153 varies from 4.50 to 4.67 ns within the above temperature limit.

Table 2
List of the bimolecular quenching constants (k_q^{TR}) and free energy changes (ΔG^0) along with other redox and energy parameters for different coumarin–amine systems in TX-100 micellar solution

Coumarin	Donor	E_{00} (eV)	$E(C/C^-)$ (V)	$E(D/D^+)$ (V)	ΔG^0 (eV)	k_q^{TR} (10^9 M^{-1} s^{-1})[a]				
						288 K	293 K	298 K	303 K	308 K
C151 (I)	DEAN	2.85	−1.48	0.59	−0.88	1.13	1.34	1.54	1.83	2.15
C152 (II)		2.76	−1.46		−0.80	3.36	3.86	4.53	5.05	5.54
C481 (III)		2.78	−1.52		−0.76	4.70	5.27	5.74	6.42	7.23
C522 (IV)		2.67	−1.51		−0.66	1.11	1.23	1.33	1.67	2.02
C153 (V)		2.61	−1.54		−0.56	1.06	1.29	1.40	1.72	1.93
C151 (I)	DMAN			0.63	−0.84	1.13	1.29	1.41	1.82	2.23
C152 (II)					−0.77	2.64	3.08	3.57	4.12	4.71
C481 (III)					−0.72	3.71	4.22	4.76	5.29	5.87
C522 (IV)					−0.62	1.26	1.43	1.57	1.91	2.29
C153 (V)					−0.52	1.08	1.26	1.43	1.69	1.99

[a] The error limit in the k_q values is ±5%.

all the coumarin–amine systems studied, and thus validates our analysis procedure to obtain the average quenching constant k_q^{TR}. The k_q^{TR} values thus estimated for different coumarin–amine pairs at different temperatures are listed in Table 2.

3.2. Correlation of the quenching constants with the free energy changes of the ET reactions

Variation of the observed ET rates with the free energy changes (ΔG^0) of the reactions is one of the very interesting aspect to investigate, especially to see if the observed variation shows an inversion at higher exergonicity region, as predicted in Marcus ET theory [1–15]. For the present systems, ΔG^0 values were calculated using Rehm–Weller relation as [61],

$$\Delta G^0 = E\left(\frac{A}{A^+}\right) - E\left(\frac{C}{C^-}\right) - E_{00} - \frac{e^2}{\varepsilon_s r_0} \quad (5)$$

where $E(A/A^+)$ and $E(C/C^-)$ are the oxidation and reduction potentials of amines and coumarins, respectively, E_{00} the excitation energy of the coumarin dyes in the S$_1$ state, e the charge of an electron, ε_s the static dielectric constant of the reaction medium and r_0 is the separation between the interacting coumarin and amine molecules. The $E(A/A^+)$ and $E(C/C^-)$ values in TX-100 micelle at ambient temperature ($\sim$298 K) were taken from our earlier work and are listed in Table 2 [40]. Since the temperature coefficients for redox potentials are usually not that large, for the limited temperature range studied (288–308 K) we approximately assume the values to remain similar. The E_{00} values of the coumarins were obtained from the intersecting wavelengths of the normalized (peak intensities) fluorescence and excitation spectra and are also listed in Table 2. In the temperature range studied, there is no observable change in the shape and position of the emission spectra. Accordingly the E_{00} values were considered to be similar at all the temperatures studied. As inferred in Section 3.1, the polarity of the microenvironment around the probe in the micellar Palisade layer remains more or less similar for the temperature range studied. Thus, the same ε_s value of $\sim$22.4 [49,62] is considered for the Palisade layer of TX-100 micelle for all the temperatures studied. For the estimation

of r_0, the radii of the coumarin dyes and amine donors were calculated using Edward's volume addition method [63], and r_0 was considered to be equal to the sum of the radii of the interacting amines and coumarin molecules [39–41]. Such an approximation does not cause any significant error in the estimated ΔG^0, as the contribution of the Coulomb term $e^2/\varepsilon_s r_0$ (cf. eq. (5)) in the estimated ΔG^0 values is quite less. For different coumarin–amine systems, the ΔG^0 values thus estimated in TX-100 micelles following the above considerations are listed in Table 2. In the present work, since our systems belong to the outer-sphere ET reactions, it is quite expected that the temperature effect on the ΔG^0 values will not be that significant [1–15]. Temperature effect on the ΔG^0 values in ET reactions mainly arises from the entropy term $-T\Delta S^0$. In charge shift reactions, from temperature dependent studies it has been shown by Closs and co-workers [64] that due to smaller contribution of the $-T\Delta S^0$ term, the ΔG^0 values are not that significantly dependent on temperature. For the present charge separation reactions also similar situation is supposed to be quite applicable, especially when the temperature ranges studied in the present work is quite limited. As suggested by Torieda et al. [65], under the condition of small nuclear displacements, the effect of anharmonicity of the vibrational modes on the intramolecular reorganization energy λ_i is not that significant. Under this situation, the λ_i for the ET reactions can be considered to be almost temperature independent [65]. For coumarin–aromatic amine systems, under nondiffusive intermolecular ET conditions, the intramolecular reorganization energy is understood to be not that high ($\sim$0.2 to 0.3 eV [40,66]). Thus, it is reasonable to consider λ_i to be effectively temperature independent for these systems. As the polarity of the microenvironment around the coumarin probes in TX-100 micelle is seen to remain almost similar for the temperature range studied [49], solvent reorganization energy λ_s can also be considered to be effectively temperature independent [31,67]. Based on the above considerations, we assume that the ET parameters for the present systems do not change to any significant extent with temperature, at least for the small temperature range studied in the present work.

Typical Marcus correlation plots for the ET rates versus the reaction exergonicity ($-\Delta G^0$), as obtained for different
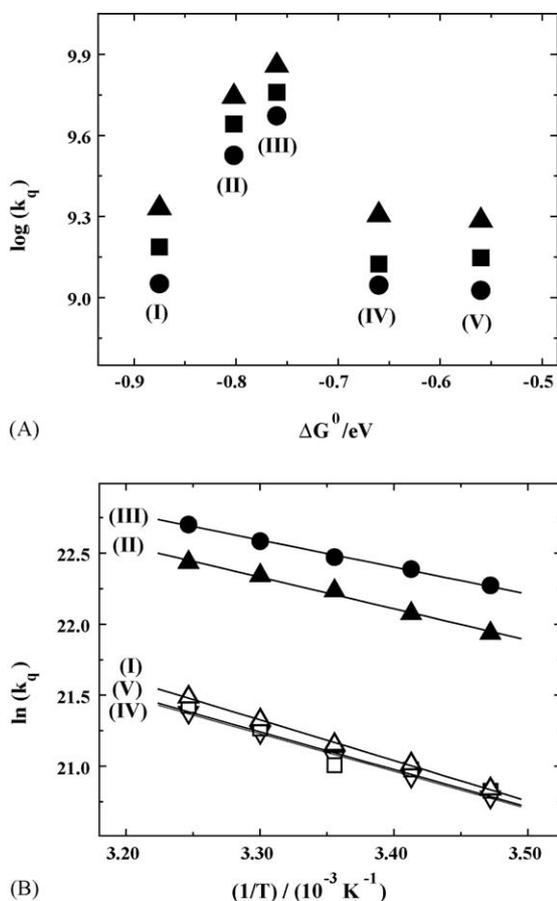
Fig. 2. (A) Marcus correlation plots for the ET rates in the coumarin–DEAN systems with the free energy changes of the reaction at different temperatures: 288 K (●), 298 K (■) and 308 K (▲). Inversion in the ET rates apparently occurs at around 0.75 eV. Data points corresponding to different coumarin dyes are indicated by Roman numbers I–V, in accordance with Table 2. (B) Arrhenius plots for different coumarin–DEAN pairs. It is seen that the plot for C481 dye at the apparent activation less region (III, symbol ●) show lower activation barrier compared to those of C522 (IV, symbol ▽) and C153 (V, symbol □) dyes in the normal region and C152 (II, symbol ▲) and C151 (I, symbol △) dyes in the inverted regions.

Table 3
Activation energies for different coumarin–aromatic amine pairs

Coumarins	ΔE (kcal mol^{-1})	
	DEAN	DMAN
C151 (I)	5.72	5.94
C152 (II)	4.11	5.12
C481 (III)	3.80	4.08
C522 (IV)	5.29	5.28
C153 (V)	5.28	5.40

Another important point to be mentioned here that in correlating the quenching constants with ΔG^0 values, we always relied on the average fluorescence lifetimes τ_{av} to estimate the k_q^{TR} values. As discussed earlier, due to statistical distribution of the quenchers around the fluorophore in the micelle, fluorescence decays were expected to follow a nonexponential behavior. Accodingly, the individual τ_1 and τ_2 components of the fluorescence decays, as we obtained by approximating the decays as a biexponential function, can not be assigned separately to any particular distribution of the fluorophore–quencher pairs in the micelle. Thus, we feel that the use of τ_1 and τ_2 components independently to estimate one fast and one slow quenching contants for the present systems will not carry any physical meaning. On the contrary, use of τ_{av} gives the estimate of the average quenching constants which is quite meaningful to give the average picture of the micellar ET systems.

For the present systems, it is seen that within experimental error, the temperature dependent k_q^{TR} values correlate well with the Arhenius type of correlation [68], where $\ln k_q^{TR}$ varies linearly with $1/T$. Typical Arrhenius plots for coumarin–DEAN pairs are shown in Fig. 2B. From the Arrhenius plots, the activation energies (ΔE) have been calculated for different coumarin–aromatic amine pairs and are listed in Table 3. From these temperature dependent results following interesting points can be noted. (1) For all the coumarin amine pairs, independent of ΔG^0, the k_q^{TR} values are temperature dependent and follow the linear Arrhenius type of correlation. (2) Though the activation barrier is much higher for the coumarin amine pairs that are either in the normal or in the inverted region and quite away from the maxima of the Marcus correlation plots, the activation energy for the coumarin amine pairs that are very close to the maxima of the correlation plots ($-\Delta G^0 \sim 0.75$ eV) are also quite significant. (3) With an increase in the temperature, the Marcus correlation plots gradually move upwards without showing any apparent change in the shapes of the correlations. According to the conventional ET theory [1–15], maximum ET rate should appear at the barrierless condition ($-\Delta G^0 = \lambda_s + \lambda_i$) and this ET rate should be temperature independent. Temperature effect on the ET rates in the true inverted region ($-\Delta G^0 > \lambda_s + \lambda_i$) is also expected to be quite insignificant due to the participation of nuclear tunneling involving the high frequency vibrational modes [10,11,31,69–71]. In the normal region, however, ET rate should be strongly temperature dependent, as the free energy of activation is nonzero and there will not be any nuclear tunneling. Therefore, if the observed inversion in the Marcus correlation plots for the present system was true inversion as expected from

coumarin–DEAN pairs at different temperatures are shown in Fig. 2A. Similar correlation plots were also obtained for different coumarin–DMAN pairs studied in the present work. For all the temperatures, these plots indicate an inversion in the ET rates (Marcus inversion behavior) around an exergonicity of about 0.75 eV, as are also reported in our earlier works on micellar ET reactions [39–41]. To be mentioned here that in Fig. 2A, unlike in our earlier report [40], we do not go for any quantitative correlation of the k_q^{TR} values with ΔG^0, as the k_q values are quite largely fluctuating in the higher ΔG^0 region and accordingly we do not expect to obtain any meaningful values for the ET parameters from such correlations, especially as a function of temperature. Thus, in the present paper we discuss the results mainly in a qualitative manner, to understand the temperature effect on the ET rates in micellar solution. As indicated from Fig. 2A, Marcus inversion in the ET rates is evident beyond an exergonicity of about 0.75 eV, for all the temperatures studied.

conventional ET theories [1–15], almost no temperature effect was expected at the exergonicities corresponding to the maxima as well as the inverted region ($-\Delta G^0 > \sim 0.75$ eV). Present results with substantial temperature effect even in the inverted region indicate that there is no nuclear tunneling involved for the present systems. As inferred in our earlier studies [39–41], the observed Marcus inversion in micellar ET reactions arises due to slow solvation dynamics, which effectively causes a partial contribution of the solvent reorganization energy λ_s in determining the free energy of activation following 2DET model [42]. Thus, inversion in the Marcus correlation plots in micellar ET systems seems to be an apparent inversion rather than true inversion expected normally beyond the barrierless condition of $-\Delta G^0 = \lambda_s + \lambda_i$. Accordingly, for the present systems, not only the coumarin–amine pairs that are at the maxima of the Marcus correlation plots but also those in the observed inverted region in Fig. 2A actually correspond to the conditions of $-\Delta G^0 < \lambda_s + \lambda_i$, which is truly the normal region on the basis of the conventional ET theories. Thus, high frequency vibrational modes are not expected to be involved in these systems, resulting the ET rates to be significantly temperature dependent.

In the present systems, observed temperature effect even for the coumarin–amine pairs close to the maxima of the Marcus correlation plots (cf. Fig. 2A) indicates that these maxima are not at the true barrier-less condition of $-\Delta G^0 = \lambda_s + \lambda_i$. It is indicated from Fig. 2A that the maxima in the Marcus correlation plots for the ET rates appear approximately at an exergonicity of ~ 0.75 eV, which is quite low in comparison to the total reorganization energy expected for the present systems. Thus, considering the polarity of the Palisade layer of TX-100 micelle, the solvent reorganization energy λ_s is expected to be in the range of about 1.1 eV [40]. For coumarin–aromatic amine systems, λ_i is also expected to be ~ 0.2–0.3 eV [40,66]. Thus, it is evident that the onset of Marcus inversion in the ET rates for the present systems occurs at a substantially lower exergonicity (cf. Fig. 2A) than expected. In micellar solution, it is understood from earlier studies that the solvent relaxation process is comparatively slower than the ET reaction and thus ET dynamics is not that significantly influenced by solvation dynamics [39–41]. Moreover, under the situation of slow solvation, the reactant state always remains in a nonequilibrium solvent configuration during the progress of the ET reaction and this causes the λ_s to contribute only partially to the free energy of activation [39–41,66,67]. Accordingly, the inversion in the Marcus correlation plots for these systems occurs at an exergonicity much lower than true barrier less condition [39–41], making it to be an apparent inversion.

Under the condition of slow solvent relaxation, as envisaged from 2DET theory [42], the effective fraction λ_s^{eff} of λ_s that contributes to the free energy of activation is related to the nonequilibrium solvation coordinate X_g by the following relation [39–41,66,67]:

$$\lambda_s^{eff} = \lambda_s(1 - 2X_g) \tag{6}$$

Though an exact estimate of X_g is not possible, a rough estimate can be obtained from the differences in the Stocks' shifts $\Delta(\Delta\nu)$

of the coumarin dyes between micellar solution and a nonpolar solvent (negligible dielectric relaxation), by using the following relation [5,66,67]:

$$2\lambda_s X_g^2 = \Delta(\Delta\nu) \tag{7}$$

Considering the present micelle and a nonpolar solvent cyclohexane, the average $\{\Delta(\Delta\nu)\}$ value for the coumarin dyes is estimated to be ~ 1400 cm^{-1}. Thus, considering $\lambda_s \sim 1.1$ eV in TX-100 micelle [40], an X_g value is estimated to be about 0.28. Using this X_g value, λ_s^{eff} is estimated to be ~ 0.48 eV for the present ET systems. This λ_s^{eff} value in addition to the expected λ_i of about 0.2–0.3 eV [40,66], thus, roughly accounts for the exergonicity of ~ 0.75 eV as observed for the maxima of the Marcus correlation plots in the present systems (cf. Fig. 2A). These correlations, though quite approximate, yet indicate that the solvent relaxation process does not significantly affects the ET rates in the present systems. Accordingly, present results are in support of the applicability of the 2DET model for the micellar ET reactions [39–41].

According to 2DET model, ET can occur along intramolecular coordinate q for any solvent coordinate X. Following this model, the ET reactions in the present systems can be schematically represented in terms of the free energy surfaces as in Fig. 3A or in terms of the free energy contours as in Fig. 3B [39–42]. As a general description, the dependence of the ET rate constant on different ET parameters can be expressed by the following equation [1–15]:

$$k_{et} = \frac{2\pi}{\hbar} V_{el}^2 (4\pi\lambda k_B T)^{-1/2} \exp\left(\frac{-\Delta G^*}{k_B T}\right) \tag{8}$$

where $\hbar$ is the Planck constant divided by 2π, V_{el} the electronic coupling matrix element which is determined by the extent of overlap between the reactant and the product electronic wave functions, k_B the Boltzman constant, T the absolute temperature and ΔG^* is the free energy of activation for the ET reaction. Incorporating the concept of 2DET theory [42], the free energy of activation ΔG^* is not only the function of ΔG^0, λ_s and λ_i, but also a strong function of X_g, the nonequilibrium solvation coordinate for the reactant state [5,66,67]. If it is assumed that the ET reaction along q occurs much faster than the solvent reorganization dynamics, then the X_g, as it appears for the reactant state immediately after the photoexcitation will not change much and thus the free energy of activation ΔG^* should be expressed as [5,66,67],

$$\Delta G^*(X) = \frac{[\lambda_s(1 - 2X) + \Delta G^0 + \lambda_i]^2}{4\lambda_i} \tag{9}$$

In photoinduced ET reaction, as are the present cases, it is quite likely that X_g can be quite away from the equilibrium solvent coordinate ($X = 0$). As discussed in the previous paragraph, a rough estimate gives an X_g value of about 0.28 for the present systems, which suggests a substantial displacement of the reactant state from the equilibrium solvent coordinate. Thus, under the situation of very slow solvent relaxation, only $(1 - 2X_g)$ fraction of λ_s (cf. Eq. (6)) can only effectively contribute in determining $\Delta G^*(X)$. Accordingly, the inversion in the
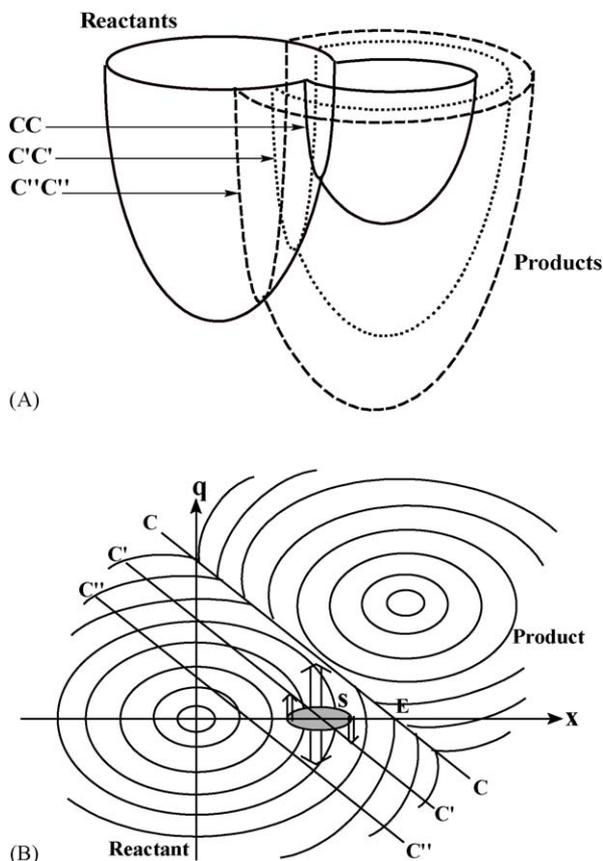
Fig. 3. (A) Qualitative free energy (FE) surface crossings between reactant and product states at different exergonicities of the ET reactions, as envisaged from 2DET theory. (B) Isoenergy contours of the FE surfaces drawn in a two-dimensional plane for the reactant and product states in relation to the 2DET theory. The TS curves corresponding to different ΔG^0 are indicated by CC, C'C', C''C''.

Marcus correlation plots should appear at an exergonicity much lower than the total reorganization energy of $\lambda_s + \lambda_i$, and obviously much before the condition of the true barrierless situation is reached.

In Fig. 3A and B, the free energy crossing curve CC between the reactant and the product states is the actual transition state (TS) curve for the 2DET reaction. To be mentioned that on the basis of conventional ET theory, the single crossing point E on the solvation axis X in Fig. 3B should represent the unique TS for the ET reaction. In microheterogeneous systems like micelles, it is reported that the solvent relaxation dynamics are drastically retarded in comparison to that in homogeneous solutions [48,49,56,72]. In our earlier ET studies using coumarin–aromatic amine systems in SDS and TX-100 micelles it is indicated that the solvation rates in these micelles are either slower or at the most comparable to the observed ET rates [39–41]. Therefore, in these micellar solutions, following 2DET theory, a nonequilibrium solvation condition for the reactant state will always be prevailed during the progress of the ET reaction along q, as the initial reactant state is produced with a solvent coordinate X_g which is substantially away from the equilibrium solvent coordinate. Hypothetically assuming that the point S in Fig. 3B represents the nonequilibrium solvent coordinate X_g for

the reactant state, the ET results in the present systems can be explained on the basis of the following considerations. Suppose that the CC curve in Fig. 3B represents the TS curve for the 2DET in the present systems at a particular ΔG^0 value. If the ΔG^0 is now changed towards higher exergonicities, the TS curve will gradually shift to the new positions, namely C'C', C''C'', etc. With C'C' situation, as the TS curve crosses X axis at S, at this exergonicity the ΔG^* along q will be effectively zero, causing the ET rate to become the maximum, even though the reaction exergonicity is still less than that of the true barrier-less condition. According to Fig. 3B, the true barrier-less condition should correspond to the TS curve passing trough the origin of the plot ($q = 0$ and $X = 0$). For the exergonicity conditions on either side of the C'C' situation, e.g. the cases corresponding to the CC and C''C'' curves, respectively, the ΔG^* becomes nonzero and thus causes lower ET rates with significant temperature dependence expected. Accordingly, in the Marcus correlation plots, the CC and C''C'' situations should appear in the apparent normal and inverted regions, respectively, with the maxima representing the C'C' situation. Considering the TS curve C'C' in Fig. 3B, the ΔG^* should be zero only for an ideal situation, where the reactant state is confined to the single point S. In reality, however, the reactant state will have a reasonably wide distribution along X, as qualitatively shown by the black semicircle around S in Fig. 3B. Moreover, since the solvent relaxation process is not completely frozen in the present systems (cf. average solvation times $\langle \tau_s \rangle$ are listed in Table 1), during the progress of the ET reaction the broadness for the distribution of the reactant state along X is supposed to be increased to some extent with time. Accordingly, the ET rates even at the maxima of the Marcus correlation plots in Fig. 2A are expected to show some temperature effect, rather than showing complete temperature independence. However, the temperature effect near the maxima of the Marcus correlation plots is expected to be relatively less than those at the other exergonicities for the observed normal and inverted region. Observed temperature effects for the present ET systems thus support the above predictions. As indicated from Table 2, the estimated activation barrier for the coumarin–amine pairs closer to the maxima of the Marcus correlation plots (point III) is about 30% less than that of the values estimated for the other coumarin–amine pairs either in the observed normal region (points IV and V) or in the inverted region (points I and II).

Following conventional ET theory, the ET rates at the true barrierless condition should be temperature independent. In the true inverted region also, due to nuclear tunneling the ET rates was expected to be almost temperature independent [10,11,31,69–71]. Reasonable activation barrier observed for all the coumarin–amine pairs, irrespective of their position in the Marcus correlation plots, thus indicates that the inversion observed in the present systems is not the true inversion. We therefore infer that the Marcus inversion observed in the present ET systems in micellar solution is in fact an apparent inversion and occurs at exergonicities much lower than normally expected. Based on 2DET theory we infer that this apparent inversion in the present systems arises due to the slow solvent relaxation dynamics in the present systems [39–41]. Thus, according to Fig. 3, at exergonicity corresponding to the TS curve C'C', it gives the

apparent maxima in the Marcus correlation plots, even though the exergonicity $-\Delta G^0$ is less than $\lambda_s + \lambda_i$. For exergonicities higher than this, and till the TS curve pass through the origin of the plot ($q = 0$ and $X = 0$), exergonicities are less than the true barrier-less situation. We feel that the data points in the inverted region of the observed Marcus correlation plots in Fig. 2A are in fact in the region of $-\Delta G^0 < \lambda_s + \lambda_i$, because for the similar coumarin–aromatic amine systems no inversion was observed even in the ultrafast ET studies, and thus these systems were indicated to be in the normal region of the reaction exergonicity [5,66,67].

While considering the temperature effect on the observed ET rates, it is very important to know the temperature effect on the parameters like the free energy change ΔG^0 and the reorganization energies, λ_s and λ_i [69–71]. Following 2DET theory, the temperature dependent rate equation for ET reaction along q should be explicitly written as [5,7,66–71],

$$k_{et}(T) = \frac{2\pi}{\hbar} \frac{V_{el}^2}{\sqrt{4\pi\lambda_i(T)k_B T}} \exp\left[-\frac{\{\Delta H^0(T) - T\,\Delta S^0(T) + \lambda_s(T)[1 - 2X_g] + \lambda_i(T)\}^2}{4\lambda_i(T)k_B T}\right] \tag{10}$$

At an arbitrary temperature T, even though the entropy term $-T\Delta S^0$ is supposed to shift the ΔG^0 towards a negative value, for a small temperature range investigated in the present work, and with the expectation that the ΔS^0 for the outer-sphere ET reactions is not that large, the effect of the entropy term to ΔG^0 may be considered to be quite small. For the present systems, temperature effect on the λ_s and λ_i values are also expected to be not that large as discussed previously. Thus, the observed temperature effect in the present ET systems is reasonably explained on the basis of the 2DET theory. Presents results also support our earlier inference that the observed Marcus inversion in the micellar ET reactions is in fact an apparent inversion, arising due to the slow solvent relaxation in micellar media in comparison to the ET rates. It is important to mention here that a true Marcus inversion for ET reaction must appear at an exergonicity higher than the solvent reorganization energy [1–15]. For the present cases, as the inversion appears much below the solvent reorganization energy (1.1 eV) as estimated considering the polarity of the micellar Palisade layer [40], it must be an apparent inversion observed for these systems. This is an unique observation of apparent Marcus inversion even though the ET systems belong to the normal exergonicity region.

4. Conclusion

ET in coumarin–amine systems in TX-100 micellar solution shows inversion in the Marcus correlation plots for the observed ET rates with the reaction exergonicities. Interestingly, it is seen that the onset of the Marcus inversion in the present systems appears at exergonicity, which is much lower in comparison to the total reorganization energy in these systems. This observation is rationalized on the basis of the 2DET theory, considering a faster ET rate along nuclear coordinate q, as the relaxation along solvent coordinate X is comparatively slower. Present results indicate that the observed Marcus inversion in the ET rates in micellar solutions is in fact an apparent

inversion and appears much before the true barrier-less situation of $-\Delta G^0 = \lambda_s + \lambda_i$. The temperature dependent results on the ET dynamics in coumarin–aromatic amine systems in TX-100 micellar solution also support the inference that the inversion observed in the Marcus correlation plots is an apparent inversion. It is understood that the temperature effect on the ET rates in the present systems arises due to the activation barrier for the ET reaction along q, and the contribution of solvent reorganization energy in this barrier is only partial, due to a persisting nonequilibrium solvent reorganization for the reactant state during the ET reaction. Present results provide a supportive evidence for our earlier inference from micellar ET studies [39–41] that the 2DET model is more suitable to explain the ET results in these heterogeneous media than the conventional ET theories. The most important finding of the present study is the appearance of the Marcus inversion in the ET rates even at an exergonicity that is much lower than the true barrierless situation.

References

[1] J.R. Durrant, S.A. Haque, E. Palomares, Coord. Chem. Rev. 248 (2004) 1247.
[2] J.M. Mayer, Annu. Rev. Phys. Chem. 55 (2004) 363.
[3] K.R. Rodgers, G.S. Lukat-Rodgers, Compr. Coord. Chem. II 8 (2004) 17.
[4] J. Jortner, M. Bixon (Eds.), Electron Transfer From Isolated Molecules to Biomolecules, Wiley, New York, Adv. Chem. Phys. 106–107 (1999) 1.
[5] K. Yoshihara, K. Tominaga, Y. Nagasawa, Bull. Chem. Soc. Jpn. 68 (1995) 696.
[6] H. Heitele, Angew. Chem. Int. Ed. Engl. 32 (1993) 359.
[7] G.J. Kavarnos, Fundamentals of Photoinduced Electron Transfer, VCH Publishers, New York, 1993.
[8] M.A. Fox (Ed.), Electron Transfer: A Critical Link Between Subdisciplines in Chemistry, Special Issue on Electron Transfer, Washington, D.C., Chem. Rev. 92 (1992) 365.
[9] J.R. Bolton, N. Mataga, G.L. McLendon (Eds.), Electron Transfer in Inorganic, Organic and Biological Systems, American Chemical Society, Washington, DC, 1991.
[10] M.D. Newton, N. Sutin, Annu. Rev. Phys. Chem. 35 (1984) 437.
[11] R.A. Marcus, N. Sutin, Biochem. Biophys. Acta 811 (1985) 265.
[12] I. Rips, J. Jortner, J. Chem. Phys. 87 (1987) 2090.
[13] I. Rips, J. Jortner, J. Chem. Phys. 87 (1987) 6513.
[14] R.A. Marcus, J. Chem. Phys. 24 (1956) 966.
[15] R.A. Marcus, J. Chem. Phys. 24 (1956) 979.
[16] G.L. Closs, J.R. Miller, Science 240 (1988) 440.
[17] J.R. Miller, L.T. Calcaterra, G.L. Closs, J. Am. Chem. Soc. 106 (1984) 3047.
[18] G.L. Closs, L.T. Calcaterra, N.J. Green, K.W. Penfield, J.R. Miller, J. Phys. Chem. 90 (1986) 3673.
[19] I.R. Gould, S. Farid, Acc. Chem. Res. 29 (1996) 522.
[20] H. Segawa, C. Takehara, K. Honda, T. Shimidzu, T. Asahi, N. Mataga, J. Phys. Chem. 96 (1992) 503.
[21] J.R. Scott, A. Willie, M. McLean, P.S. Stayton, S.G. Stigar, B. Durham, M. Francis, J. Am. Chem. Soc. 115 (1993) 6820.
[22] E. Vauthey, J. Phys. Chem. A 105 (2001) 340.
[23] I.R. Gould, D. Noukakis, L. Gomez-Jahn, J.L. Goodman, S. Farid, J. Am. Chem. Soc. 115 (1993) 4405.
[24] I.R. Gould, D. Ege, J.E. Moser, S. Farid, J. Am. Chem. Soc. 112 (1990) 4290.

[25] H. Segawa, C. Takehara, K. Honda, T. Shimidzu, T. Asahi, N. Mataga, J. Phys. Chem. 96 (1992) 503.

[26] T. Kakitani, N. Mataga, J. Phys. Chem. 90 (1986) 993.

[27] T. Ohno, A. Yoshimura, N. Mataga, J. Phys. Chem. 90 (1986) 3296.

[28] G. Grampp, Angew. Chem. Int. Ed. Engl. 32 (1993) 691.

[29] E. Prasad, K.R. Gopidas, J. Am. Chem. Soc. 122 (2000) 3191.

[30] S. Fukuzumi, K. Ohkubo, H. Imahori, D.M. Guldi, Chem. Eur. J. 9 (2003) 1585.

[31] D.M. Guldi, K.D. Asmus, J. Am. Chem. Soc. 119 (1997) 5744.

[32] S. Fukuzumi, Y. Yoshida, T. Urano, T. Suenobu, H. Imahori, J. Am. Chem. Soc. 123 (2001) 11331.

[33] K. Weidemaier, H.L. Tavernier, M.D. Fayer, J. Phys. Chem. B 101 (1997) 9352.

[34] K. Weidemaier, H.L. Tavernier, K.T. Chu, M.D. Fayer, Chem. Phys. Lett. 276 (1997) 309.

[35] H.L. Tavernier, A.V. Barzykin, M. Tachiya, M.D. Fayer, J. Phys. Chem. B 102 (1998) 6078.

[36] H.L. Tavernier, F. Laine, M.D. Fayer, J. Phys. Chem. A 105 (2001) 8944.

[37] C.D. Clark, M.Z. Hoffmann, Coord. Chem. Rev. 159 (1997) 359.

[38] A.A. Alkaitis, G. Beck, M. Gratzel, J. Am. Chem. Soc. 97 (1975) 5723.

[39] M. Kumbhakar, S. Nath, H. Pal, A.V. Sapre, T. Mukherjee, J. Chem. Phys. 119 (2003) 388.

[40] M. Kumbhakar, S. Nath, T. Mukherjee, H. Pal, J. Chem. Phys. 120 (2004) 2824.

[41] M. Kumbhakar, S. Nath, T. Mukherjee, H. Pal, J. Chem. Phys. 122 (2005) 084512.

[42] H. Sumi, R.A. Marcus, J. Chem. Phys. 84 (1986) 4894.

[43] S. Fukuzumi, M. Nishimine, K. Ohkubo, N.V. Tkachenko, H. Lemmetyinen, J. Phys. Chem. B 107 (2003) 12511.

[44] K. Streletzky, J.D. Philies, Langmuir 11 (1995) 42.

[45] G.B. Dutt, J. Phys. Chem. B 106 (2002) 7398.

[46] K. Kalyansundaram, Photochemistry in Microheterogeneous Systems, Academic Press, Orlando, 1987.

[47] H.H. Paradies, J. Phys. Chem. 84 (1980) 599.

[48] M. Kumbhakar, S. Nath, T. Mukherjee, H. Pal, J. Chem. Phys. 121 (2004) 6026.

[49] M. Kumbhakar, T. Goel, T. Mukherjee, H. Pal, J. Phys. Chem. B 108 (2004) 19246.

[50] J.B. Birks, Photophysics of Aromatic Molecules, Wiley–Interscience, New York, 1970.

[51] P.P. Infelta, M. Gratzel, J.K. Thomas, J. Phys. Chem. 78 (1974) 190.

[52] P.P. Infelta, M. Gratzel, J. Chem. Phys. 78 (1983) 5280.

[53] M. Tachiya, Chem. Phys. Lett. 33 (1975) 289.

[54] M. Tachiya, Can. J. Phys. 68 (1990) 797.

[55] M. Tachiya, in: G.R. Freeman (Ed.), Kinetics of Non-Homogeneous Processes, Wiley, New York, 1987.

[56] S.K. Pal, A. Datta, D. Mandal, K. Bhattacharya, Chem. Phys. Lett. 288 (1998) 793.

[57] J.A. Dean (Ed.), Lange's Handbook of Chemistry, 13th ed., McGraw-Hill, New York, 1987.

[58] S. Nad, H. Pal, J. Chem. Phys. 116 (2002) 1658.

[59] S. Nad, H. Pal, J. Phys. Chem. A 104 (2000) 673.

[60] W.J. Albery, P.N. Bartlett, C.P. Wilde, J.R. Darwent, J. Am. Chem. Soc. 107 (1985) 1854.

[61] D. Rehm, A. Weller, Israel J. Chem. 8 (1970) 259.

[62] M. Kumbhakar, S. Nath, T. Mukherjee, H. Pal, J. Chem. Phys. 121 (2004) 6026.

[63] J.T. Edwards, J. Chem. Edu. 47 (1970) 261.

[64] N. Liang, J.R. Miller, G.L. Closs, J. Am. Chem. Soc. 111 (1989) 8740.

[65] H. Torieda, A. Yoshimura, K. Nozaki, S. Sakai, T. Ohno, J. Phys. Chem. A 106 (2002) 11034.

[66] H. Shirota, H. Pal, K. Tominaga, K. Yoshihara, J. Phys. Chem. A 102 (1998) 3089.

[67] Y. Nagasawa, A.P. Yartsev, K. Tominaga, A.E. Johnson, K. Yoshihara, J. Chem. Phys. 101 (1994) 5717.

[68] P.W. Atkins, Physical Chemistry, Oxford University Press, Oxford, 1994.

[69] N. Liang, J.R. Miller, G.L. Closs, J. Am. Chem. Soc. 112 (1990) 5353.

[70] J. Kroon, H. Oevering, J.W. Verhoeven, J.M. Warman, A.M. Oliver, M.N. Paddon-Rows, J. Phys. Chem. 97 (1993) 5065.

[71] K.J. Smit, J.M. Warman, M.P. de Haas, M.N. Paddon-Row, A.M. Oliver, Chem. Phys. Lett. 152 (1988) 177.

[72] K. Bhattacharyya, B. Bagchi, J. Phys. Chem. A 104 (2000) 10603.